

MICRODEVICES IN MEDICINE¹

Dennis L. Polla, Arthur G. Erdman, William P. Robbins,
David T. Markus, Jorge Diaz-Diaz, Raed Rizq, Yunwoo
Nam, and Hui Tao Brickner

*Department of Biomedical Engineering, University of Minnesota, Minneapolis,
Minnesota 55455; e-mail: polla@ece.umn.edu*

Amy Wang and Peter Krulevitch

*Center for Microtechnology, Lawrence Livermore National Laboratory, Livermore,
California 94550; e-mail: wang24@llnl.gov*

Key Words microelectromechanical systems, MEMS, bioMEMS,
microfabrication, microsystems, biosensors, mass spectrometer, stepper motor,
piezoelectricity, surgical microsystems, diagnostic microsystems, therapeutic
microsystems

■ **Abstract** The application of microelectromechanical systems (MEMS) to medicine is described. Three types of biomedical devices are considered, including diagnostic microsystems, surgical microsystems, and therapeutic microsystems. The opportunities of MEMS miniaturization in these emerging disciplines are considered, with emphasis placed on the importance of the technology in providing a better outcome for the patient and a lower overall health care cost. Several case examples in each of these areas are described. Key aspects of MEMS technology as it is applied to these three areas are described, along with some of the fabrication challenges.

CONTENTS

INTRODUCTION	552
Enabling Technologies	552
Technology Assessment and Directions	553
SURGICAL MICROSYSTEMS	553
Surgical Microsensors	558
Surgical Micromotors	559
DIAGNOSTIC MICROSYSTEMS	562
Miniature Mass Spectrometers	563
Molecular-Recognition Biosensors	563
Microfluidic Processors	566

¹The US Government has the right to retain a nonexclusive, royalty-free license in and to any copyright covering this paper.

THERAPEUTIC MICROSYSTEMS	567
Implantable Drug Delivery Microsystems	568
Transdermal Drug Delivery Microsystems	569
CONCLUSIONS	572

INTRODUCTION

Biomedical microelectromechanical systems (bioMEMS) apply the same manufacturing methods that are used in making computer microchips to making ultrasmall medical sensors, actuators, and motors (1, 2). These tiny devices, also referred to as biomedical microsystems, hold promise for precision surgery with micrometer control, rapid screening of common diseases and genetic predispositions, and autonomous therapeutic management of allergies, pain, and neurodegenerative diseases. The health care implications predicted by successful development of this technology are enormous, including early identification of disease and risk conditions, less trauma and shorter recovery times, and more accessible health care delivery at a lower total cost.

This review is not intended to exhaustively cover all of the numerous bioMEMS works that have been published to date. Rather, we present an introduction to the technology, provide general references to the literature, and describe representative biomedical microsystems, primarily from work at the University of Minnesota and Lawrence Livermore National Laboratory, that exemplify emerging opportunities in medicine. In particular, three rapidly developing areas of microsystems technology present enormous opportunities for research and commercialization: (a) diagnostic microsystems, (b) surgical microsystems, and (c) therapeutic microsystems. Given the research missions of our organizations, we have selected project examples that convey the excitement of merging developments in microelectromechanical systems (MEMS) technology with multiple research themes in scientific, engineering, and medical disciplines.

Enabling Technologies

Integrated-circuit (IC) processing methods have been developed and refined over the last 40 years in the manufacture of common microelectronic chips such as microprocessors and data storage or "memory." The same process technologies used in silicon microelectronic chip manufacture are also routinely used in the fabrication of MEMS and bioMEMS. Specifically, unit process steps such as thin-film deposition, photolithography, etching, and packaging have routine application to both ICs and MEMS. The use of a silicon starting-substrate material originally suggested the enormous promise of integrating both MEMS and ICs in sophisticated self-contained microsystems capable of autonomously performing intelligent functions such as sensing and signal processing, at a very low manufacturing cost.

Although the basic steps in the IC unit process are widely used in MEMS and bioMEMS fabrication, a special process known as solid-state micromachining (4, 5) represents a unique enabling method not commonly used in the production of

conventional microelectronic chips such as microprocessors or memory. In simple terms, solid-state micromachining is a method for forming a useful mechanical structure, such as a thin supported membrane (pressure sensor) or cantilever beam (accelerometer) by methods of selective material removal through a combination of etching and/or material deposition and photolithographic-patterning techniques. Two methods used to make thin, flexible diaphragms, such as those used in solid-state pressure sensors, are shown in Figure 1. These methods rely on (Figure 1, *top*) subtractive etching of the substrate material, called bulk micromachining (4) and (Figure 1, *bottom*) the addition of two or more patterned materials followed by the selective removal of one of these materials, which is temporary. This latter method is commonly referred to as surface micromachining (5).

An example of the main steps involved in surface micromachining is shown in Figure 2, for the production of a piezoelectric microcantilever beam sensor. This is a generic process to form activity monitors for pacemaker applications (6), molecular-recognition biosensors (7), and vibration-monitoring structures (8).

Technology Assessment and Directions

Although many interesting medical-device concepts based on microfabrication have been presented over the past 20 years, only a small (but growing) number of these have actually been applied in real health care settings. Possible reasons for the low adoption of these devices by the medical industry include (a) technical barriers such as roadblocks in packaging, materials, fluidics, and interconnects; (b) inadequate attention to systems requirements; (c) reliability; (d) testing, calibration, and packaging difficulties; (e) high entry and facilities development costs; (f) inertia of the medical industry; (g) the US Food and Drug Administration approval process; and (h) inadequate understanding of health care needs and the health care environment. Despite these challenges, a number of MEMS devices have made it to the marketplace, notably discrete (without on-chip electronics) pressure sensors (9) and chemical-analysis devices (10), which have become high-volume medical-sensor products. Integrated systems that contain two or more of the following components are still a significant challenge: mechanical structures, sensors, electronics, actuators, optics, and microfluidic elements (11).

A number of universities, research institutions, and corporations now have ongoing bioMEMS activity. Representative examples of these are listed in Table 1.

SURGICAL MICROSYSTEMS

Once a patient's condition has been diagnosed, treatment can involve costly and invasive surgical procedures that require significant recovery time. Often the success of procedures depends on the dexterity of individual surgeons and accessibility of remote locations in the body. A current trend in surgical procedures is toward minimally invasive surgery, an approach whereby the large and potentially traumatic incisions that have been part of conventional procedures are replaced by tiny

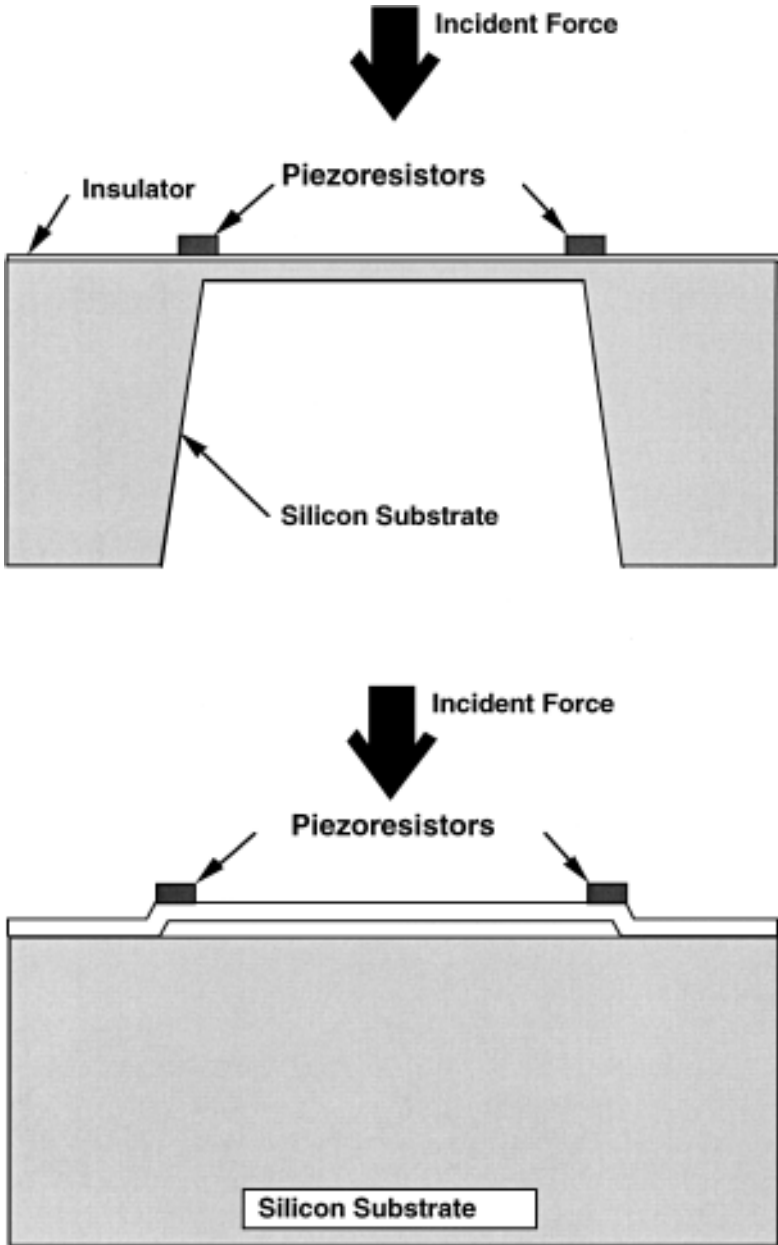


Figure 1 Two examples of solid-state micromachining. (*top*) Bulk micromachining usually involves the removal of the substrate material by chemical etching methods. (*bottom*) Surface micromachining applies the additive incorporation of several different materials followed by the selective removal of one of these materials, usually by chemical etching.

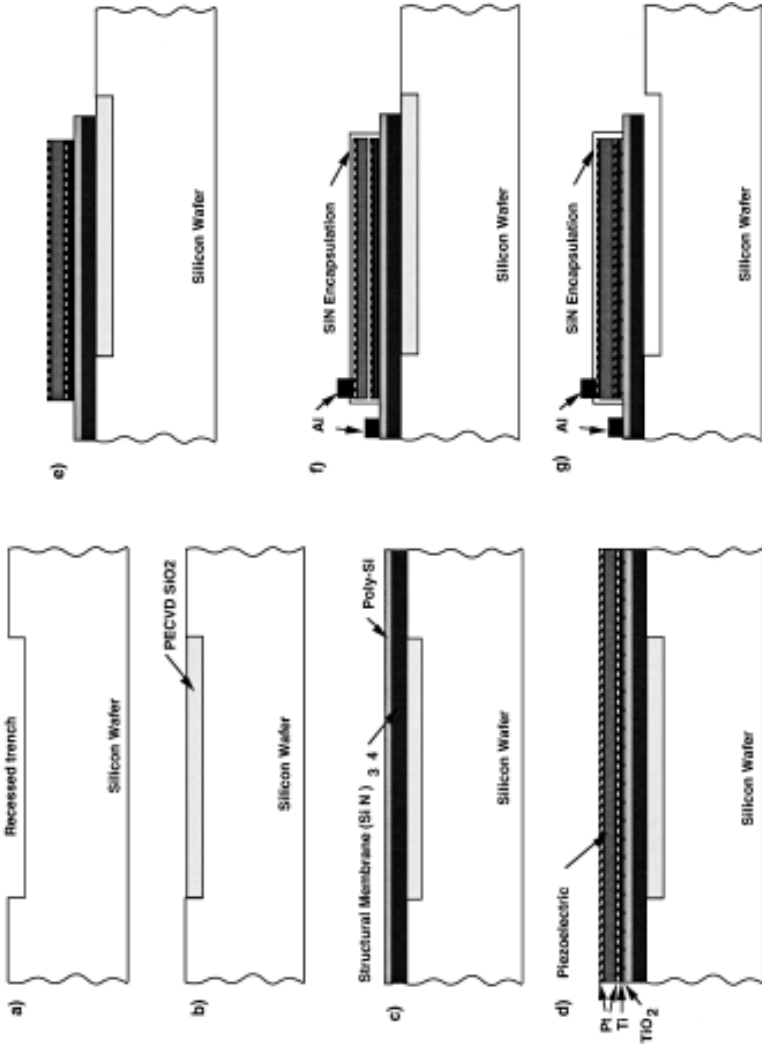


Figure 2 Representative piezoelectric microelectromechanical-systems process used to produce a microbeam vibration-monitoring device. (a) Reactive-ion etched recessed trench formation, (b) etchback planarization, (c) low-pressure chemical vapor deposition silicon nitride (structural support) and low-pressure chemical vapor deposition polysilicon (adhesion layer) depositions, (d) piezoelectric thin-film electrodes and capacitor depositions, (e) structural membrane and capacitor definitions, (f) encapsulation and metal contact formation, and (g) sacrificial etching.

TABLE 1 Representative universities, research institutions, and corporations with ongoing biomedical micromechanical systems (bioMEMS) activity

bioMEMS activity	Organization	Reference(s)
Diagnostic instruments		
DNA arrays	Affymetrix (Santa Clara, CA)	12
DNA synthesis arrays	Perkin Elmer Applied BioSystems (Foster City, CA)	13
DNA hybridization analysis arrays	Nanogen (San Diego, CA)	14
Microfluidics-based analysis systems	Cepheid (San Jose, CA)	15
Nanoliter DNA processors	University of Michigan (Ann Arbor, MI)	16
Blood cell separators	Princeton University (Princeton, NJ)	17
Capillary electrophoresis systems	University of California, Berkeley (Berkeley, CA)	18
Sorting of cells	Princeton University (Princeton, NJ)	19
Breast cancer detection	University of California, Berkeley (Berkeley, CA)	20
FPW biosensors	University of California, Berkeley (Berkeley, CA)	21
Acoustic particle manipulation	University of California, Berkeley (Berkeley, CA)	22
Capillary electrophoresis systems	Caliper Technologies (Palo Alto, CA)	23
MEMS chemical sensors and immunosensors	Case Western Reserve University (Cleveland, OH) and Ohio State University (Columbus, OH)	24–26 27, 28
High-speed sequencing instrumentation for the Human Genome Project	Lawrence Livermore National Laboratory (Livermore, CA)	27
Miniaturized PCR DNA amplification chamber	Lawrence Livermore National Laboratory (Livermore, CA)	28
Microfluidics	University of California, Santa Barbara (Santa Barbara, CA)	29
Optically based continuous-flow and separations technology	University of Washington (Seattle, WA)	30
Molecular-recognition biosensor array	University of Minnesota (Minneapolis, MN)	31
High-density droplet array for DNA processing	University of Washington (Seattle, WA)	32

(continued)

TABLE 1 (Continued)

bioMEMS activity	Organization	Reference(s)
Mass spectrometer	University of Minnesota (Minneapolis, MN)	33
Electrochemiluminescence detection	University of California, Davis (Davis, CA)	34, 35
Surface Plasmon Resonance	University of California, Davis (Davis, CA)	36, 37
Evanescant array pathogen detectors	Naval Research Laboratory (Washington, DC)	38
Contact protein printing	Harvard University (Cambridge, MA)	39, 40
Surgical instruments		
MEMS sensors on catheters	Fraunhofer Institute, Karlsruhe, Germany	
Minimally invasive devices	Cent. for Innovative Minimally Invasive Therapy, Massachusetts General Hospital (Boston, MA)	41
Microfabricated ultrasonic cutting tools	University of California, Berkeley (Berkeley, CA)/University of Wisconsin (Madison, WI)	42
Smart sensor for cataract removal	University of Minnesota (Minneapolis, MN)	6, 43
Microactuator for releasing embolic coils	Lawrence Livermore National Laboratory (Livermore, CA)	44
Therapy management		
Blood-testing systems	I-STAT Corp. (East Windsor, NJ)	45
Drug infusion micropumps	DeBiotech (Lausanne, Switzerland)	46
Chemical sensors and packaging	University of California, Davis (Davis, CA)	47
Chemical sensors	University of Washington (Seattle, WA)	48
Telemetry, home health care monitoring	University of Minnesota (Minneapolis, MN)	49
Miniaturized combinatorial chemistry for drug discovery	Affymax Research Institute (Palo Alto, CA)	50
High-throughput chemical synthesis	Orchid Biocomputer Inc. (Princeton, NJ)	51
Artificial liver, currently in clinical trials	University of Minnesota (Minneapolis, MN)	52
Neural probes	Stanford University (Palo Alto, CA)	53
Silicon neurowells	California Institute of Technology (Pasadena, CA)	54
Measurement of contractile forces on cells	University of California, Los Angeles (Los Angeles, CA)	55

incisions through which specialized instruments are inserted. Minimally invasive surgery reduces the trauma in treatment and also reduces health care cost with faster procedures and shorter hospital stays. For instance, endovascular procedures are replacing open-heart surgeries, enabling patients to return to work in a few days rather than several weeks. This same advancement can be extended to treating neurovascular diseases, in which the blood vessels are even smaller. However, smaller medical devices are required to fit through microcatheters while maintaining the flexibility to maneuver through the tortuous anatomy of the arteries. We like to think of MEMS technology as providing a new opportunity for “micro-invasive surgery.”

Surgical Microsensors

Surgical microsensors represent a relatively new application for MEMS technology. The approach described in this work uses a piezoelectric material to identify tissue properties by monitoring the impressed tissue loading on a surgical cutting tool (56). The real-time response (charge vs time or voltage vs time) provides information to the surgeon during procedures that require delicate cutting.

Cataract removal, involving an ultrasonic cutting technique called phacoemulsification, is one of the most common surgical procedures practiced in the United States, with ~1.6 million performed yearly. In this technique the hard, opaque human lens is fragmented by a sharp, ultrasonically driven cutting needle. Because the ophthalmologist cannot see directly under the hollow titanium or stainless steel cutting needle as the lens is fragmented and aspirated, the underlying and much softer posterior capsule is sometimes unintentionally ruptured. The very fragile posterior capsule is easily cut in comparison with the hard protein molecules composing the lens. A tear usually requires considerable time to repair and invariably leads to complications such as glaucoma, infection, and sometimes blindness. The complication rate of this procedure is highly dependent on the skill and experience of the surgeon.

A piezoelectric sensor (force transducer) has therefore been designed and inserted directly behind the cutting needle to actively warn the surgeon when a hard-to-soft material transition that is characteristic of the lens-to-posterior capsule transition is taking place. A diagram of such a modified surgical cutting tool is shown in Figure 3.

The physical sensing method can rely on either the direct detection of the impressed loading on the needle presented by the lens or on continuous monitoring of the natural frequency with which the system oscillates under an ultrasonic drive. This impressed loading is transduced to the piezoelectric sensor, which is placed in the surgical handpiece. For the surgical tool studied, a fundamental resonance was observed at 39.3 kHz. By monitoring the impedance amplitude signature near this frequency, one can correlate the processed sensor output with tissue hardness. This approach is summarized in Figure 4, in which a hard-to-soft tissue transition is detected in the ultrasonic cutting of the human lens. This procedure has been successfully applied in clinical trials on 252 patients.

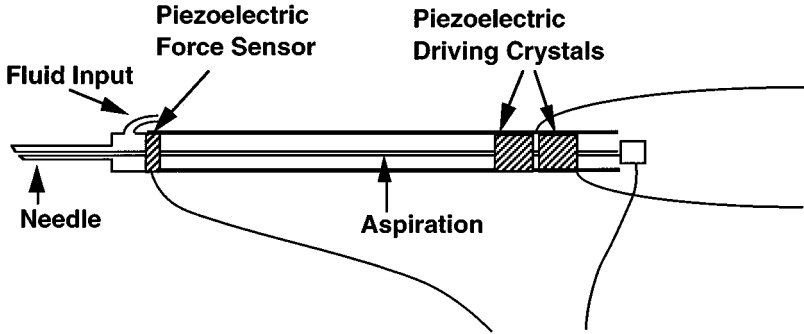


Figure 3 Piezoelectric sensor inserted into a phacoemulsification handpiece. The piezoelectric materials are designed such that the overall intended operation of the instrument is not substantially modified by the incorporation of miniature sensors.

Surgical Micromotors

A significant challenge facing the MEMS community is to ensure that effective force and useful displacement can be derived from the many physical-actuation mechanisms proposed and investigated to date. In addition, for surgical applications, small-sized, ergonomic, easy-to-use surgical devices are preferred.

A miniature piezoelectric inchworm motor (57) has been fabricated for use in a variety of precision surgical applications such as intraocular delivery of a replacement lens after cataract removal. Several generations (58) of this motor have been investigated, including the one shown in Figures 5 and 6. This design has two principal components, a glider and a fixed confining rail structure that limits the movement of the glider to one dimension. Electrical power to the glider is delivered via sliding contacts, as indicated in Figure 5, and the glider moves in a series of steps (59). A single step cycle commences when the rear end (relative to the displacement direction) of the glider is immobilized against the substrate by means of the back electrostatic clamp, while the front end of the glider is unclamped. The piezoelectric extender/contractor is then extended, moving the front end of the glider forward. The front end of the device is then clamped to the substrate by a front-end electrostatic clamp. The back-end electrostatic clamp is then deactivated, and the piezoelectric bar is allowed to contract by application of the opposite polarity of electric field across the piezoelectric material, thus moving the rear end of the glider forward. Deactivation of the front clamp and activation of the rear clamp positions the glider for another stepping sequence.

The displacement per step, δ_s , assuming that no external force is applied to the glider, and the maximum force, F_{\max} , that the glider can exert on an external load ($\delta_s = 0$) are given by Equation 1 (60):

$$\delta_s = (Ld_{13}V_{pzt}/t_{pzt}) \quad \text{and} \quad F_{\max} = Ewd_{13}V_{pzt} \quad (1)$$

If the glider is clocked f_s times per second, then the stepping rate or movement

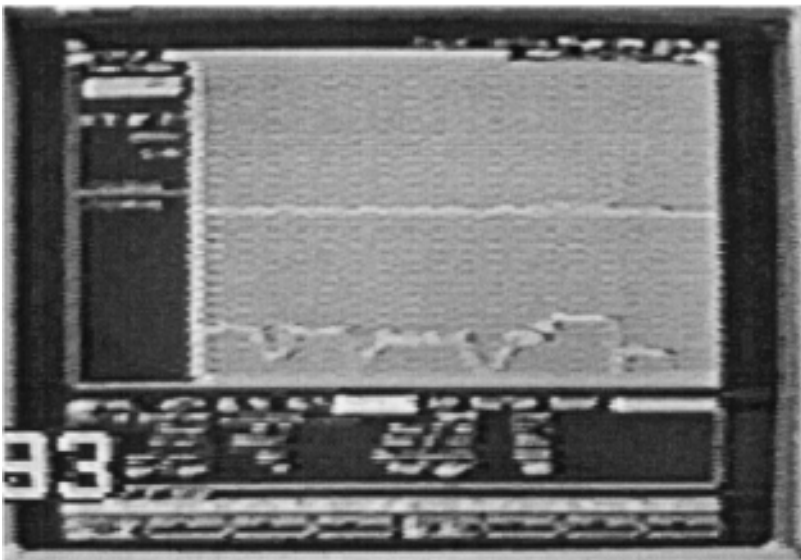
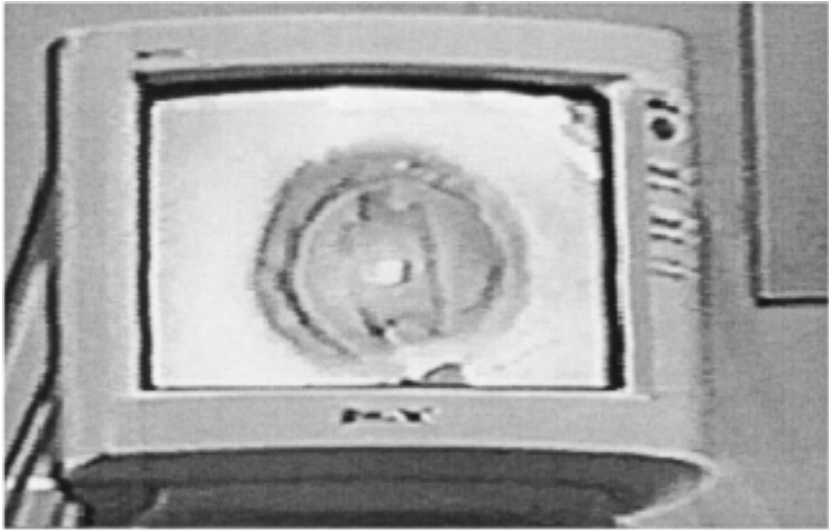


Figure 4 Piezoelectric sensor waveform captured during the removal of the live human lens. The reduction in sensor amplitude indicates a hard-to-soft tissue signature to alert the surgeon about the possible breakage of the posterior capsule.

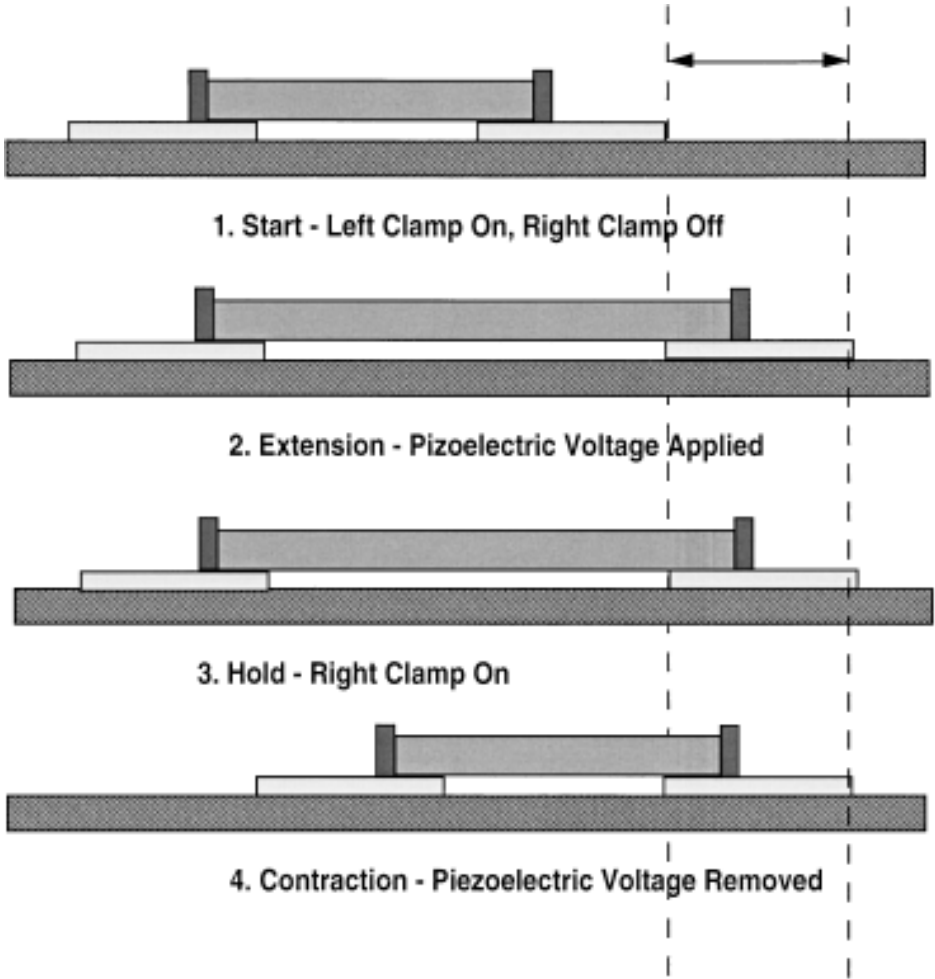


Figure 5 Four-step operation of the piezoelectric inchworm motor. (1) Clamping to immobilize back end of motor, (2) piezoelectric extension, (3) clamping of front end, and (4) release of back end and piezoelectric contraction.

velocity is $f_s L d_{13} V_{pzt} / t_{pzt}$, assuming that $L = 200 \mu\text{m}$, $w = 50 \mu\text{m}$, $t_{pzt} = 0.5 \mu\text{m}$, and $V_{pzt} = 2V$, $\delta_s = 0.2 \mu\text{m}$, and $F_{\text{max}} = 1.9 \times 10^{-3} \text{ N}$ or $1900 \mu\text{N}$. These estimates assume that the electrostatic clamps are strong enough to keep the glider immobilized against the external applied forces.

We have fabricated several versions of inchworm stepper motors and have verified the displacement, velocity, and force performance equations (58). Clocking frequencies of several hundred hertz were used with the stepper motors, and larger

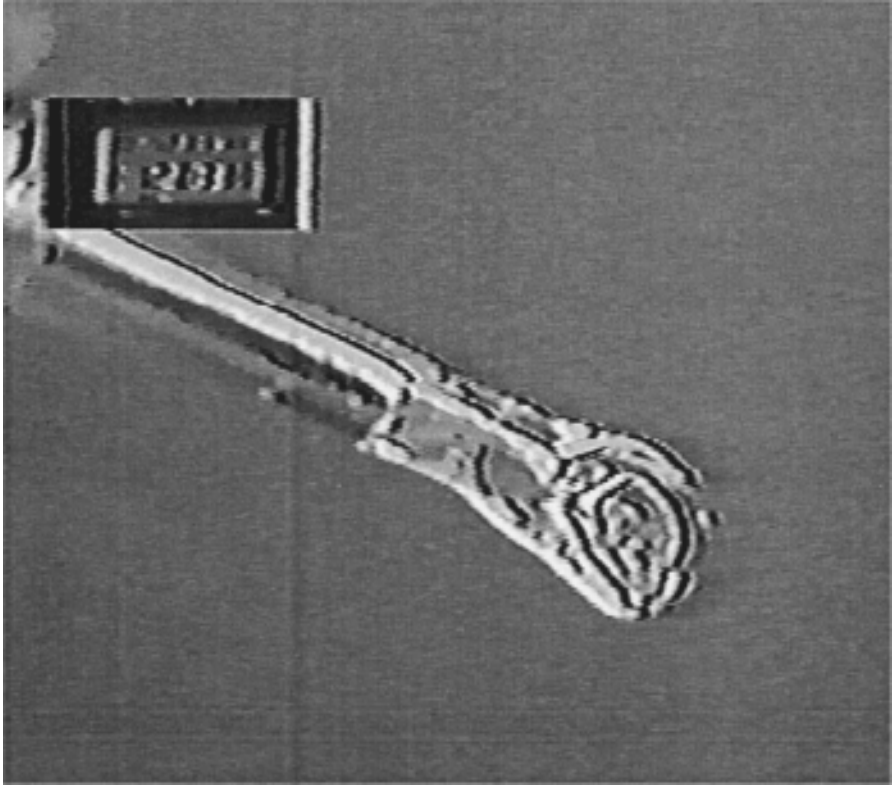


Figure 6 Application of a hand-held inchworm motor to ophthalmology. The motor incrementally advances to deploy a replacement silicone lens.

clocking frequencies should be feasible with microscale stepper motors. An optical photograph of the piezoelectric micromotor, taken at the point of delivering a silicone lens from a plastic cassette, is shown in Figure 6.

DIAGNOSTIC MICROSYSTEMS

The application of MEMS technology to diagnostic microsystems focuses on the development of new affordable instruments, based on miniaturization technologies, that are critical to the rapid and inexpensive diagnosis of disease. Examples of analytical functions that are benefitting from such developments include blood supply screening, analysis of biopsy samples and body fluids, minimally invasive and noninvasive diagnostic procedures, rapid identification of disease, and early screening. These systems will eventually perform diagnostic procedures in a multiplexed format that incorporates multiple complementary methods. Ultimately these systems will be combined with other devices to create completely integrated

analysis and treatment systems. MEMS devices or MEMS injection molding techniques may also be important in realizing inexpensive disposable bioanalytic microchips. Because this area has attracted considerable scientific interest and the commercial interest of the biotechnology industry, three representative projects are briefly described below.

Miniature Mass Spectrometers

Mass spectrometry is currently used in many biomedical applications, such as respiratory-gas monitoring, body fluid analysis, disease screening, and peptide and protein identification. Molecules of a sample are ionized, passed through electric and magnetic fields to separate the ions by their mass-to-charge ratios, and then detected. The resulting mass spectrum reflects a unique signature for a given molecular species. Both the sensitivity and resolving power of modern mass spectrometers can be extremely high, and, unlike many other analytical methods, mass spectroscopy requires relatively little advance knowledge of the sample composition. A disadvantage of current analytical-grade mass spectrometers is the relatively high costs associated with both the equipment and human handling.

A novel subminiature, double-focusing mass spectrometer for in situ gas-monitoring applications has been fabricated at the University of Minnesota by a combination of conventional machining methods and microfabrication techniques (61). Its design is based on the mass separation capabilities of a crossed electric and magnetic sector field analyzer ($r_0 = 2$ cm), which, under proper conditions, can be used to effectively cancel the angular and chromatic dispersion of the ion beam, thus achieving a significantly higher resolving power than that obtained in other mass spectrometers. The particular design also provides a very compact geometry for the overall instrument by avoiding the use of energy and mass analyzers that are placed in tandem, as is typically done with other double-focusing mass spectrometers. A photograph of the finished device is shown in Figure 7.

Ion simulations with finite element analysis and computer modeling have been used to design, verify, and optimize the performance of this instrument before its fabrication. The electric fringing-field effects, which are particularly important for small-sized mass spectrometers, were corrected by placing lithographically defined electrodes along the ion path. The fabricated lab prototype attained a resolving power of 106, a detection limit of ~ 10 ppm, and a mass range ≤ 200 amu. Its size and power consumption make this miniature mass spectrometer ideal for portable analytical instrumentation such as that potentially to be used in respiratory-gas monitoring applications at the patient's bedside. As an example, spectra obtained on air is shown in Figure 8.

Molecular-Recognition Biosensors

Biomolecular-recognition sensors have been developed for possible use in clinical laboratories, to provide cost-effective diagnostic devices that can rapidly evaluate a patient's condition with a minimum of human intervention. These devices, with



Figure 7 The main analyzer of the miniature mass spectrometer.

the appropriate chemistries, are intended to provide rapid analysis of such common disease conditions as strep throat, ovarian cancer, and genetic predispositions.

One approach taken in our laboratory is to use piezoelectric cantilever beam resonators with specific molecular-recognition coatings, as shown in Figure 9. The resonator is driven by AC voltage, using a simple-circuit technique that allows the oscillation to take place at its primary resonant frequency. Upon exposure to a conjugate biomolecule, the effective mass m at the end of the cantilever (paddle) changes by Δm . This causes the resonant frequency f of the microcantilever to shift downward by an amount Δf proportional to the change in mass given by

$$\Delta f/f = S_m \Delta m \quad (2)$$

where S_m is a proportionality constant that is dependent on beam dimensions, damping effects, etc.

The challenge of this type of device is to develop the appropriate surface coating on the end of the microcantilever—one that is both sensitive to and selective for the biomolecule of interest. This often involves the use of linker molecules to make an attachment to the standard MEMS materials composing the microcantilever.

Figure 10 shows the shift in frequency of this device in the selective binding of biotin-streptavidin. The frequency change of 12.5 kHz translates into an effective mass change of $\sim 10^{-8}$ g. This type of device is now being extended to the detection of environmental pathogens and certain types of viruses.

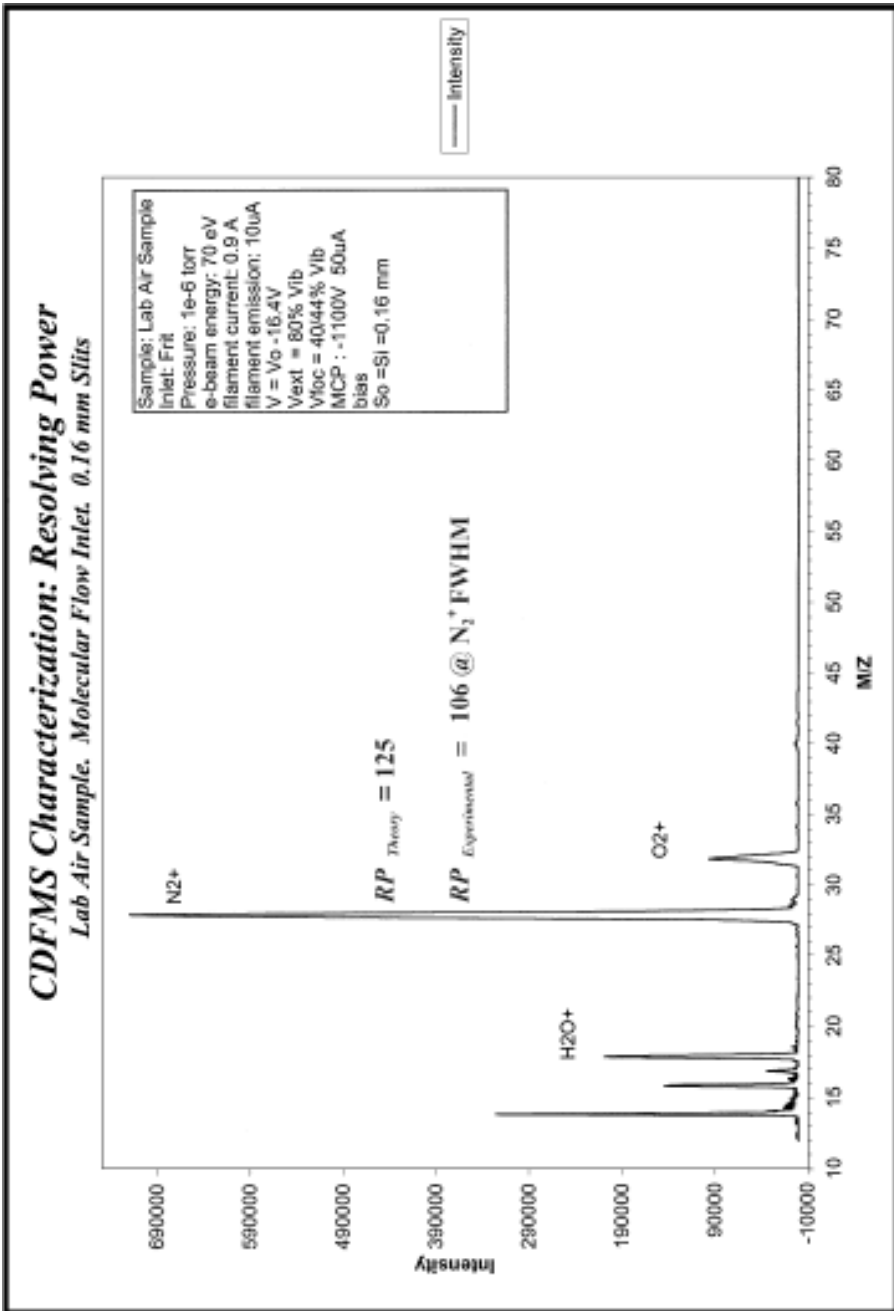


Figure 8 Representative gas spectra obtained by the miniature mass spectrometer.

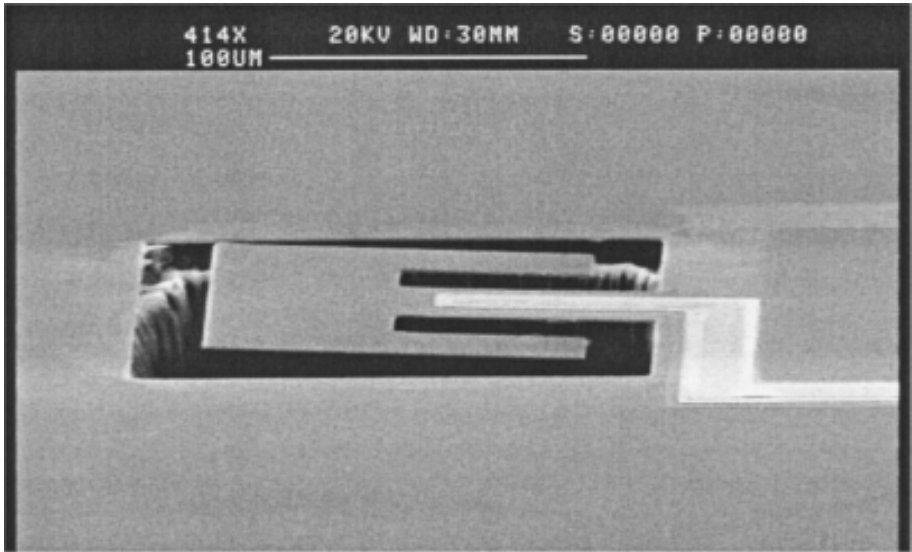


Figure 9 Scanning electron micrograph of a molecular recognition piezoelectric microcantilever.

Microfluidic Processors

In a Defense Advanced Research Projects Agency (DARPA)-sponsored collaborative research effort between MD Anderson Cancer Center and Lawrence Livermore National Laboratory, researchers are developing a microfabricated device that is capable of separating particles such as blood cells, sensing them, and identifying

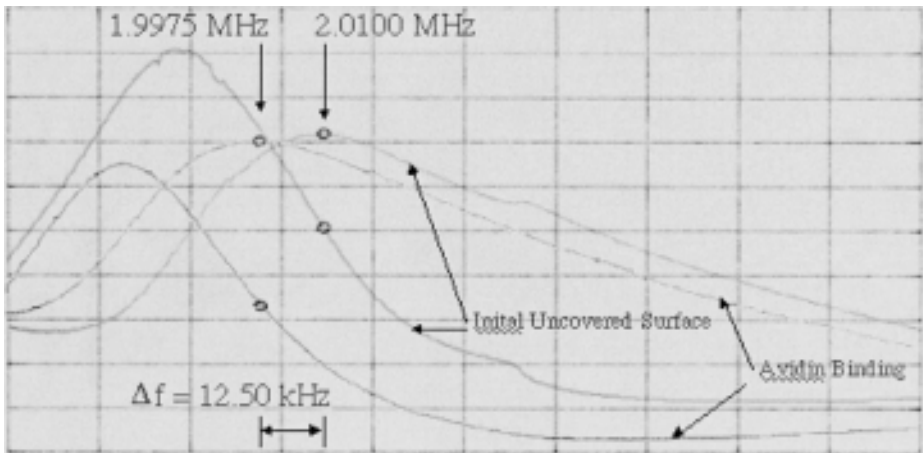


Figure 10 Shift in frequency caused by streptavidin binding on a biotin-coated piezoelectric microcantilever.

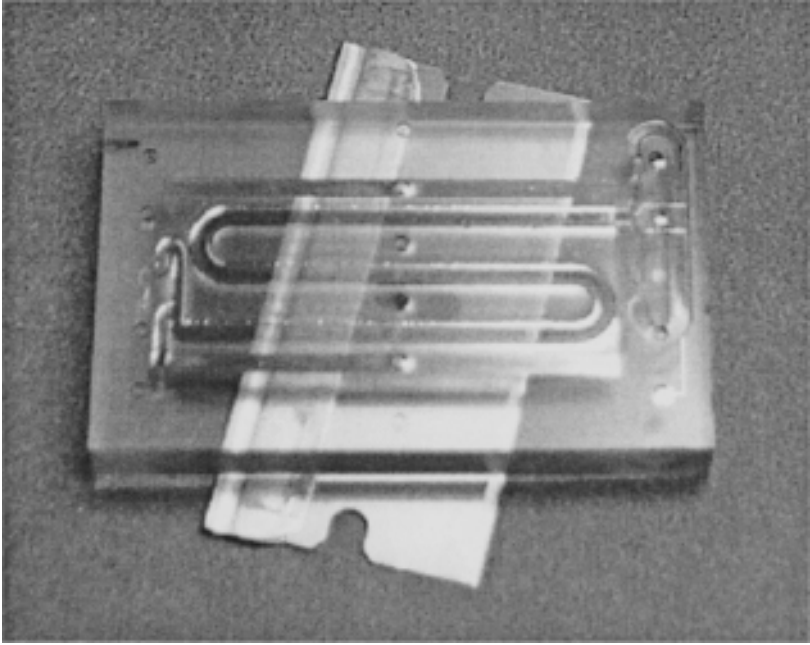


Figure 11 Cell identification device based on dielectrophoresis.

them based on their dielectric properties (62). Particularly novel in this approach is the use of impedance monitoring to spectroscopically identify the type and number of particular cells, including unhealthy cells that indicate a disease condition.

In separating the cells (known as fractionation), negative dielectrophoresis is used to keep cells levitated in a microfluidic channel and away from impedance-sensing electrodes. In passing through the microfabricated fluid columns, which measure $150\ \mu\text{m}$ deep, $1\ \text{mm}$ wide, and $10\ \text{cm}$ long (Figure 11), the cells have unique passage-time characteristics, as well as dielectric frequency spectra that allow for both counting and identification (63). In operation, a micropump sends $1\text{-}\mu\text{l}$ samples of human cells into the microchannel. The samples are then slowly flushed through the fluid from another small reservoir. The cells are detected as they pass an array of impedance sensor electrodes after fractionation along the channel.

THERAPEUTIC MICROSYSTEMS

Many chronic medical conditions can be managed by having the patient take specific drugs at specific dose levels on a regular/periodic basis. For example, cancer pain, nonmalignant pain, severe spasticity associated with multiple sclerosis, spinal

cord injury, cerebral palsy, and traumatic brain injury are now routinely treated by means of implantable drug delivery systems. Sustained-release drug delivery systems provide the medicinal effects with higher efficiency and longer duration than traditional tablet dosages. In particular, they avoid the “hill and valley” phenomena associated with oral drug ingestion and provide the optimal concentration of the drug over a longer period of time. There are a number of mechanisms to provide timed release of drugs, such as microencapsulation, transdermal patches, and implants. The current state-of-the art includes systems that are approximately the size of a hockey puck, have a limited battery lifetime of ~3–7 years, and rely on the use of power-consumptive electromagnetic dispensing of fixed amounts of medication at programmed intervals, regardless of body need. Among these techniques, implantable pumps have the advantage that the drug therapy can be delivered at the optimal time and concentration to a specific site. MEMS systems combine miniature size, which is amenable to implantability, low power requirements, and the potential to precisely meter fluid samples.

Implantable Drug Delivery Microsystems

One of the key components in an implantable drug delivery system is the miniature fluid-dispensing system or micropump. By surface micromachining techniques, piezoelectric thin films based on the lead zirconate titanate (PZT) materials system have been deposited on silicon nitride structural membranes that completely seal a cavity in the silicon substrate beneath the membrane, as shown in Figure 12. When the diaphragm deflects upward or downward owing to an applied electric field across the piezoelectric thin film, the volume of the sealed cavity changes, and, if the entrance and exit channels have valves, then the structure can function as a micropump (64). Simple estimates of the performance of such a pump can be obtained by considering the pump in Figure 12 to be a circular membrane of thickness h and radius a . For simplicity we assume that the silicon nitride structural membrane and PZT have the same thickness (each $h/2$) and Young's modulus E . If a voltage V is applied to the PZT film with piezoelectric coefficient d , the unloaded (i.e. no opposing pressure) change in volume, ΔVol , of the cavity and the maximum pressure P_{max} (assuming an equal and opposite pressure so that the net deflection of the membrane is zero) generated by the pump are given by

$$\Delta\text{Vol} = \frac{3a^4(5 + 2\mu)(1 - \mu)d_{13}V}{4h^2(3 + 2\mu)} \quad \text{and} \quad P_{\text{max}} = \frac{6Ehd_{13}V}{(3 + \mu)a^2} \quad (3)$$

If $V = 10\text{ V}$, $a = 100\ \mu\text{m}$, $h = 1\ \mu\text{m}$, and Poisson's ratio $\mu = 0.3$, then $\Delta\text{Vol} = 8 \times 10^{-4}\ \mu\text{l}$, and $P_{\text{max}} = 3.4 \times 10^4\ \text{Pa}$. If the pump were driven at $\sim 1\ \text{kHz}$, the pumping speed would be $\sim 1\ \mu\text{l/s}$. These estimates are optimistic because they assume that the membrane is attached to the substrate with a very compliant attachment (in the language of the theory of plates, the edges of the membrane are simply supported).

Different investigators have explored several versions of such micropumps. At the University of Minnesota, such pumps have been fabricated by using silicon nitride membranes 100–400 μm in diameter and 1.5 μm thick with 0.35 μm of

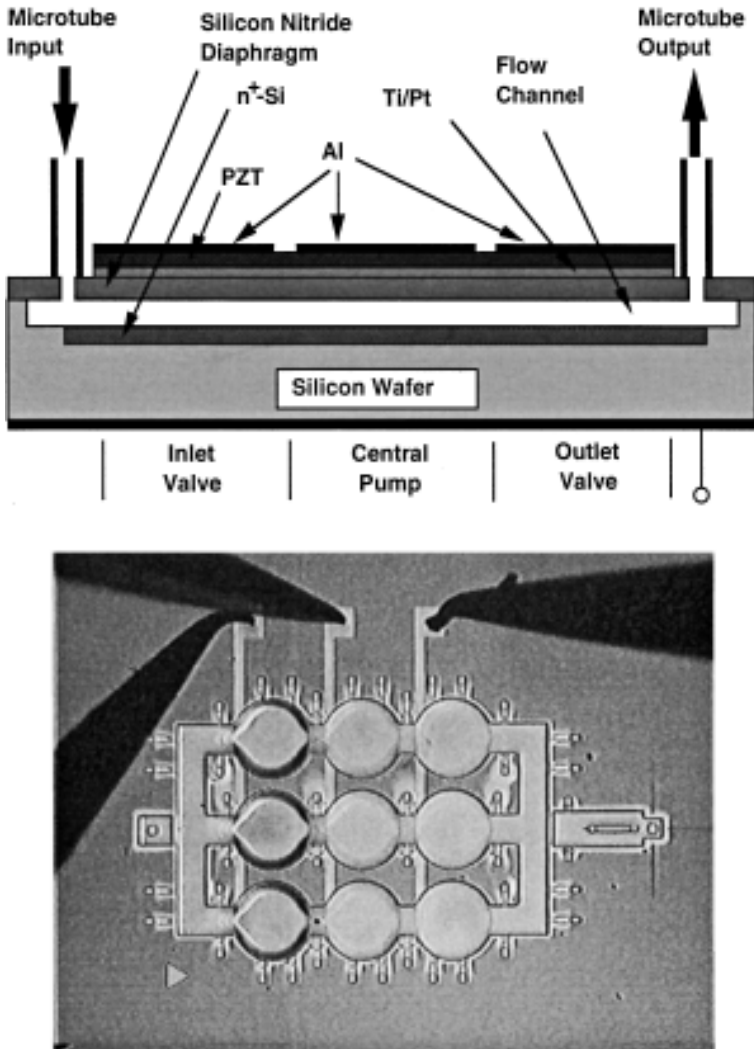


Figure 12 (top) Cross section and (bottom) photograph of a microelectromechanical-systems-based microfluidic pump. The three-stage design operates as a peristaltic pump. Each diaphragm measures $300\ \mu\text{m}$ in diameter.

PZT deposited on the top (64). The pumps can be ganged together in both series and parallel arrangements to increase the throughput and pressure differential.

Transdermal Drug Delivery Microsystems

Conventional drug delivery techniques that rely on pills and injections are often not suitable for new protein-based, DNA-based, and other therapeutic compounds produced by modern biotechnology (65). The potential of using the skin as an

alternative route for administering systematically active drugs has attracted considerable interest in recent years (66). The advantages of transdermal (across skin) drug delivery include the absence of degradation in the gastrointestinal tract and of first-pass effects in the liver, both of which are associated with oral drug delivery, and elimination of the pain and inconvenience of intravenous injection (65). The efficiency of transdermal drug delivery, however, is greatly limited by the low permeability of the human skin. The stratum corneum, which is responsible for skin impermeability, is well known for its function as a protective barrier against the loss of physiologically important substances and against the diffusion of potentially toxic chemicals from the external environment into the body (66). Generally, the stratum corneum layer is permeable only to small, lipophilic molecules. A variety of technologies have been used to controllably, reversibly, and safely reduce the resistance of the skin, thereby enhancing skin permeability. These techniques include chemical-penetration enhancers, iontophoresis, and sonophoresis (66). However, the mechanisms of each of these approaches are far from being fully understood, which limits how thoroughly the issues of feasibility and optimization can be addressed. Below we present a novel approach to transdermal drug delivery that is expected to greatly enhance the delivery efficiency. The greatest advantage of our approach is that the mechanisms of drug permeation through skin do not affect the delivery efficiency.

Skin is made of three layers: stratum corneum, viable epidermis, and dermis. The stratum corneum layer is basically a layer of dead tissue that forms a membrane, which provides the biggest barrier to drug transport. The stratum corneum is $\sim 10\text{--}15\ \mu\text{m}$ thick. Underneath the stratum corneum layer is the viable epidermis layer, which is $50\text{--}100\ \mu\text{m}$ thick. Inside this layer, there is tissue containing living cells and nerves, but no blood vessels. Deeper down is the dermis layer, which forms the bulk of skin volume and contains living cells, nerves, and blood vessels. As suggested by Henry et al (65), microneedles that penetrate the skin just a little more than $10\text{--}15\ \mu\text{m}$ should provide transport pathways across the stratum corneum that are painless, because the microneedles do not reach nerves found in deeper tissue.

The material that we use to fabricate these needles is SU-8, a negative-tone, epoxy-type, near-UV photoresist based on SU-8 resin (Shell Chemical, Houston, TX), which was originally developed by IBM. It has been demonstrated that SU-8 can be used to build structures as thick as 2 mm with aspect ratios ≤ 18 , by using standard contact photolithography. We obtained SU-8 from MicroChem Corporation (Newton, MA). The SU-8 needles were spin-coated onto a silicon substrate and patterned by standard contact photolithography. The length of the SU-8 layer is made to be either $180\ \mu\text{m}$ or $50\ \mu\text{m}$, which determines the length of the needles. The thickness of these needles can be varied easily by simply changing the concentration of the SU-8 solution and the spin speed. Needles of four different dimensions were fabricated. Channels were etched through the silicon substrate to provide a liquid-flow path. Deep reactive-ion etching (Deep Trench Etcher, Plasma-Therm, Inc.) was used to etch straight and tall channels inside silicon.

A combination of photoresist and silicon dioxide has been used as the masking material to etch silicon. The SU-8 needles were made in a 3×3 array format, as were the flow channels in silicon. The dimensions of the channels in silicon were chosen to be slightly smaller than the dimensions of the SU-8 needles that are positioned directly above them.

SU-8-based needles offer several advantages over those fabricated by silicon (67). First, there are channels built inside these needles that offer the flow path for drug transport. This is certainly the greatest advantage of this approach over any of the existing transdermal drug delivery methods. The amount of drug that is transported through the skin is no longer limited by the permeability of the skin. On the other hand, the flow is totally controlled by the external pumping mechanism. By fine-tuning the dimensions of the needles and/or the flow speed of the drugs, one can deliver drugs in a precise and controllable manner. Second, the process is straightforward, because it involves only coating and patterning of the SU-8 layer on a supporting substrate, using the well-developed photolithography technique. In this case, the supporting substrate is a silicon wafer. Third, SU-8 is nonbrittle, which greatly reduces the risk that needle tips will break inside the human skin. Fourth, SU-8 is inexpensive compared with silicon. In addition, injection molding techniques can be adopted to mass produce these needles, thus to further reduce costs. Finally, these needles can be integrated with a micropump to yield a fully integrated wristwatch type of drug delivery system. The integrated system will offer convenience, efficiency, and painlessness.

Scanning electron microscopic pictures of one of the arrays (array 2) of the microfabricated SU-8 needles are provided in Figure 13. Dark-colored liquid was observed to emerge inside the SU-8 needles as the liquid was being pushed from the other side of the silicon substrate, which demonstrates that the channels built inside the SU-8 needles are open and serve as a fluid pathway. The mechanical-strength tests of these needles were performed on human skin specimens provided by the Tissue Procurement Facility of the Cancer Research Center at the University of

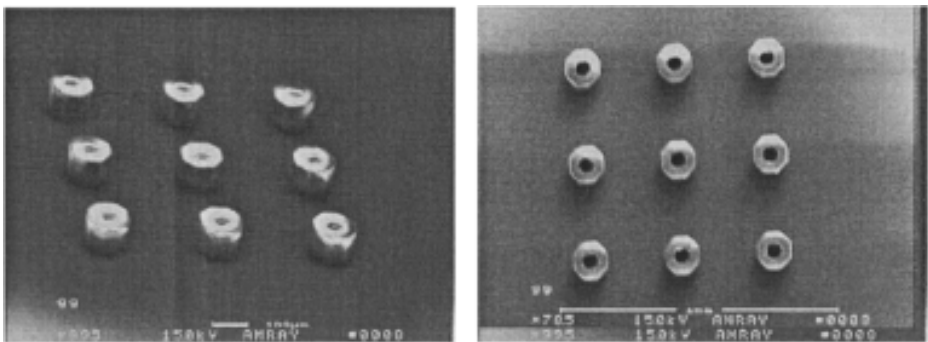


Figure 13 Scanning electron microscopic images of the needles (array 2) on silicon substrate. (Left) Side view; (right) top view.

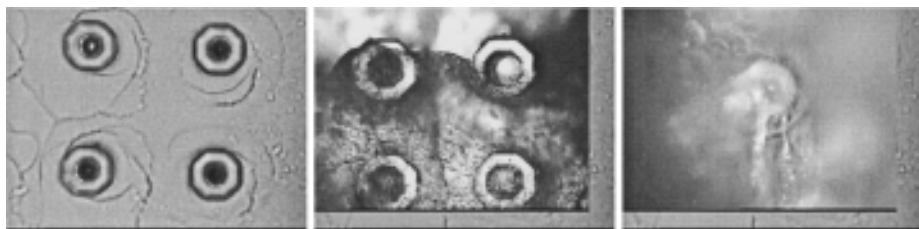


Figure 14 (*left*) Microscopic image of the needles (array 2) after the mechanical-strength test. The epidermis layer was peeled off the needles. (*center*) Top view microscopic image of array 2. The images were taken after the needles were pushed into an epidermis layer, with an epidermis layer on top and (*right*) side view.

Minnesota. The epidermis layer was separated from the bulk skin by a standard heat procedure (68). We used only the epidermis for the mechanical-strength test, for the following reasons. First, the primary barrier for molecular transport is the stratum corneum. Second, most drugs *in vivo* would be taken up by capillaries found near the dermal-epidermal junction (65). Arrays of microneedles were pushed into the skin by a thumb, just like pushing a pin into a wall. Bulk skin was placed underneath the epidermis to serve as a cushion and also to better simulate the *in vivo* mechanical environment. Then the needles, along with the epidermis layer, were removed from the bulk skin and examined under a microscope. Finally, the epidermis layer was peeled from the needles. The needles were once again examined under the microscope to determine whether their structures remained intact. The preliminary mechanical-test results can be summarized as follows. First, all of the needles that we examined remained intact after the skin test, as demonstrated by Figure 14, which shows array 2 under a microscope. Second, none of the needles were observed to pierce through the epidermis layer. Figures 14 (*left*) and 14 (*center*) are microscopic images of array 2 after it has been pushed into an epidermis layer. It was qualitatively observed that the needles stretched the epidermis layer, as they were pushed into the epidermis. This is better demonstrated by Figure 14 (*right*), which is a tilted view of the needles with the epidermis on top. In some cases, the epidermis broke owing to stress caused by this pushing process [see Figure 14 (*center*)]. These observations suggest that the structure of the needles may not be sharp enough to allow them to penetrate through the epidermis. However, based on the experimental results we currently have, it is not clear whether the needles penetrate into the epidermis layer.

CONCLUSIONS

An exciting new revolution in medicine is just beginning to unfold in laboratories around the world. The new field of bioMEMS applies the same manufacturing methods that are used for computer microchips to making ultrasmall medical

sensors, actuators, and motors. Applications of MEMS materials and processing technologies hold the promise of inexpensive health care devices, once they are manufactured in batch quantities, similar to the effect these methods have had on the costs of silicon ICs.

ACKNOWLEDGMENTS

This work was partially supported by the Whitaker Foundation. Many graduate and post-doctoral students have contributed to the projects described. We specifically thank Drs. Joon Han Kim, Yoon Soo Young, Shayne Zurn, Li Li, Yunwoo Nam, and Gareth Hughes; and we thank Long Zhang, Alex Bonne, David Drinkwater, Kuanglun Chen, Ms. Jennifer Yi, Kyeong Rho, and Haitian Hu. This work was also partially supported by the National Science Foundation grant 9601865.

Visit the Annual Reviews home page at www.AnualReviews.org

LITERATURE CITED

1. Wise KD. 1998. Scanning the special issue on integrated sensors, microactuators, and microsystems (MEMS). *Proc. IEEE* 86: 1531–33
2. Gabriel KJ. 1998. Microelectromechanical systems. *Proc. IEEE* 86:1534–35
3. Maluf N. 2000. *An Introduction to Microelectromechanical Systems Engineering*, pp. 1–265. Norwood, MA: Artech House
4. Petersen KE. 1978. Dynamic micromechanics in silicon: techniques and devices. *IEEE Trans. Electron Devices* 25:1241–50
5. Howe RT. 1988. Surface micromachining for microsensors and microactuators. *J. Vac. Sci. Technol. B* 6:1809–13
6. Kim JH, Wang L, Zurn SM, Li L, Yoon YS, Polla DL. 1997. Fabrication process of PZT piezoelectric cantilever unimorphs using surface micromachining. *Integr. Ferroelectr.* 15:325–32
7. Polla DL, Markus DT, Robbins WP, Tao H. 2000. Piezoelectric devices and MEMS. *Int. Symp. Integr. Ferroelectr., Rheinisch-Westfalische Technische Hochschule, Aachen, Germany, March 13*, p. 47
8. Polla DL, Francis LF. 1998. Processing and characterization of piezoelectric materials and integration into microelectromechanical systems. *Annu. Rev. Mater. Sci.* 28:563–97
9. Esashi M, Sugiyama S, Ikeda K, Wang Y, Miyashita H. 1998. Vacuum-sealed silicon micromachined pressure sensors. *Proc. IEEE* 86:1627–39
10. Madou MJ, Morrison SR. 1989. *Chemical Sensing with Solid State Devices*. New York: Academic. 556 pp.
11. Kovacs GTA. 1998. *Micromachined Transducers Sourcebook*, pp. 770–899. New York: McGraw-Hill
12. Anderson RC, Bogdan GJ, Puski A, Su X. 1998. Advances in integrated genetic analysis. *Micro Total Anal. Syst., 2nd*, pp. 11–16. Univ. Alberta
13. Taylor TB, St. John PM, Albin M. 1998. Micro-genetic analysis systems. *Micro Total Anal. Syst., 2nd*, pp. 261–66. Univ. Alberta
14. Cheng J, Sheldon EL, Wu L, Uribe A, Gerrue LO, et al. 1998. Electric field controlled preparation and hybridization analysis of DNA/RNA from *E. coli* on microfabricated bioelectronic chips. *Nat. Biotechnol.* 16:541–46
15. Peterson KE, McMillan WA, Kovacs GTA, Northrum MA, Christel LA, Pourahmadi F.

1998. Toward next generation clinical diagnostic instruments: scaling and new processing paradigms. *Biomed. Microdevices* 1:71–80
16. Brahmasandra SN, Johnson BN, Webster JR, Handique K, Burke DT, et al. 1998. A microfabricated fluidic reaction and separation system for integrated DNA analysis. *Micro Total Anal. Syst., 2nd*, pp. 267–70. Univ. Alberta
 17. Carlson RH, Gabel C, Chan S, Austin R. 1997. Self-sorting of white blood cells in a lattice. *Phys. Rev. Lett.* 15:2149–52
 18. Wooley AT, Mathies RA. 1994. Ultra-high-speed DNA fragment separations using microfabricated capillary array electrophoresis chips. *Proc. Natl. Acad. Sci. USA* 91:11348–52
 19. Carlson RH, Gabel C, Chan S, Austin RH. 1998. Activation and sorting of human white blood cells. *Biomed. Microdevices* 1:39–48
 20. Wang AW, Kiwan R, White RM, Ceriani RL. 1998. A silicon-based ultrasonic immunoassay for detection of breast cancer antigens. *Sens. Actuators B* 49:13–21
 21. Grate JW, Wenzel SW, White RM. 1990. Flexural plate wave devices for chemical analysis. *Anal. Chem.* 63:1222–23
 22. Meng AH, Wang AW, White RM. 1999. Ultrasonic sample concentration for microfluidic systems. *Proc. Int. Conf. Solid-State Sensors Actuators, 10th, Sendai, Jpn*, pp. 247–51. Piscataway, NJ: IEEE
 23. Bousse L, Minalla A, Deshpande M, Greiner KB, Gilbert JR. 1999. Optimization of sample injection components in electrokinetic microfluidic systems. *IEEE Int. Microelectromechanical Syst. Conf., 12th, Orlando, FL*, pp. 309–14. Piscataway, NJ: IEEE
 24. Chiem N, Colyer C, Harrison DJ. 1997. Microfluidic system for clinical diagnostics. *IEEE Int. Conf. Sensors Actuators, Chicago*, p. 183
 25. Manz A, Becker H. 1997. Parallel capillaries for high throughput in electrophoretic separations and electroosmotic drug discovery systems. *IEEE Int. Conf. Sensors Actuators, Chicago*, p. 915
 26. Madou M, Joseph J. 1993. Immunosensors with commercial potential. *Immunomethods* 3:134–52
 27. Northrup MA, Gonzalez C, Hadley D, Hills RF, Lander P, et al. 1995. A MEMS-based miniature DNA analysis system. *Proc. IEEE Int. Conf. Solid-State Sens. Actuators, 8th, Stockholm*, pp. 764–67. Piscataway, NJ: IEEE
 28. Belgrader P, Benett W, Hadley D, Richards J, Stratton P, et al. 1999. PCR detection of bacteria in seven minutes. *Science* 284:449–50
 29. Wereley ST, Meinhart CD, Santiago JG, Adrian RJ. 1998. Velocimetry for MEMS applications. *Proc. Int. Mech. Eng. Congr. Expo., Anaheim, CA*. Fairfield, NJ: ASME
 30. Galambos P, Forster FK. 1998. Microfluidic diffusion coefficient measurement. *Micro Total Anal. Syst., 2nd*, pp. 189–92. Univ. Alberta
 31. McGlennen RC, Zurn S, Charych D, Polla DL. 1997. Molecular recognition cantilever. *Proc. Int. Symp. Integr. Ferroelectr., 9th, Sante Fe, NM*, pp. 97–100. Piscataway, NJ: IEEE
 32. Bardell R, Sharma NR, Forster NR, Afromowitz MA, Penney R. 1997. Designing high-performance micro-pumps based on no-moving parts. *ASME Int. Mech. Eng. Congr. Expo., Dallas, TX, DSC-234/HTD-354*, pp. 47–53. Fairfield, NJ: ASME
 33. Diaz-Diaz J. 1998. *Microfabricated mass spectrometer*. MS thesis. Univ. Minn. 212 pp.
 34. Smith RL, Hsueh Y-T, Collins SD, Fiaccabrino J-C, Koudelka M. 1997. Electrochemiluminescence at microelectrodes for biosensing. *BIOS 97, Symp. Micro-Nanofabr. Electro-Opt. Mech. Syst. Biomed. Environ. Appl., San Jose, CA*. Bellevue, WA: Soc. Photo Optical Instrum. Eng.

35. Hsueh Y, Collins SD, Smith RL. 1997. DNA quantification with an electrochemiluminescence microcell. *Digest, Int. Conf. Solid-State Sens. Actuators, Transducers 97, 9th, Chicago, Ill.*, Extended (Abstr.) IC3.04. Piscataway NJ: IEEE
36. Garabedian R, Gonzalez C, Richards J, Knoesen A, Spencer R, et al. 1994. Microfabricated surface-plasmon sensing system. *Sens. Actuators A* 43:202–8
37. Richards JD, Garabedian R, Gonzalez C, Knoesen A, Smith RL, et al. 1992. Surface-plasmon excitation using a polarization-preserving optical fiber and an index-matching fluid optical cell. *Appl. Opt.* 32: 2901–3
38. Ligler FS, Rowe CA, Bladerson SA, Feldstein MJ, Golden JP. 1998. Fluorescence array biosensor: biochemistry and application. *Micro Total Anal. Syst.*, '98, Banff, Canada
39. Xia YN, Qin D, Whitesides GM. 1996. Microcontact printing with a cylindrical rolling stamp: a practical step toward automatic manufacturing of patterns with submicrometer-sized features. *Adv. Mater.* 8:1015–17
40. Whitesides GM. 1997. Unconventional methods and unconventional materials for microfabrication. *Proc. Int. Conf. Solid-State Sens. Actuators, 8th, Chicago, IL*, pp. 23–24. Piscataway, NJ: IEEE
41. Yarmush ML. 1998. The future of tissue engineering. *Microsyst. Technol. Med. Biol. Program, April 16, 1998*. Cambridge, MA: Cambridge Healthtech Inst.
42. Lal A. 1998. Silicon-based ultrasonic surgical actuators. *Proc. Annu. Int. Conf. IEEE Eng., 20th, Hong Kong*, pp. 2785–90. Piscataway, NJ: IEEE
43. Costin JA. 1998. Integrated Phacoemulsification System. *US Patent No. 5733256*
44. Lee AP, Ciarlo DR, Krulevitch PA, Lehes S, Trevino J, Northrup MA. 1995. A practical microgripper by fine alignment, eutectic bonding and SMA actuation. *Proc. Int. Conf. Solid-State Sens. Actuators, 8th, Stockholm, Sweden*, pp. 326–30. Piscataway, NJ: IEEE
45. Lauks IR. 1998. Biosensors and point of care blood testing instrumentation. *Microsyst. Technol. Med. Biol.* Cambridge, MA: Cambridge Healthtech Inst.
46. Maillefer D, van Lintel H, Rey-Mermet G, Hirschi R. 1999. A high-performance silicon micropump for an implantable drug delivery system. *IEEE Int. Micro Electro Mech. Syst. Conf., 12th, Orlando, FL*, pp. 541–46. Piscataway, NJ: IEEE
47. Gonzalez C, Pan JY, Collins SD, Smith RL. 1998. Packaging technology for miniature ICD instrumentation. *Med. Dev. Diagn. Ind.* pp. 70–75
48. Jung CC, Saban SB, Yee SS, Darling RB. 1996. Chemical electrode surface plasmon resonance sensor. *Sens. Actuators B* 32:143–47
49. Laxminarayan SN, Coatrieux JL, Roux CJ, Finkelstein SM, Sahakian AV, Blanchard SM. 1997. Biomedical information technology: medicine and health care in the digital future. *Trans. Inf. Biomed.* 1:1–7
50. Schullek JR, Butler JH, Ni Z-J, Chen D, Yuan Z. 1997. A high density screening format for encoded combinatorial libraries: assay miniaturization and its application to enzymatic reactions. *Anal. Biochem.* 246:20–29
51. McBride SE, Moroney RM, Chiang W. 1998. Electrohydrodynamic pumps for high density microfluidic arrays. *Micro Total Anal. Syst.*, 2nd, pp. 45–48. Univ. Alberta
52. Nyberg SL, Shatford RA, Peshway MV, White JG, Cerra FB, Hu WS. 1993. Evaluation of a hepatocyte-entrapment hollow fiber bioreactor: a potential bioartificial liver. *Biotech. Bioeng.* 41:194–203
53. Borkholder DA, Bao J, Maluf MI, Perl ER, Kovacs GTA. 1997. Microelectrode arrays for stimulation of neural slice preparations. *J. Neurosci. Methods* 77:61–66
54. Pine J. 1998. A novel silicon neurowell for studies of neural systems in vitro and in

- vivo. *Microsyst. Technol. Med. Biol.* Cambridge, MA: Cambridge Healthtech Inst.
55. Lin G, Pister KSJ, Roos KP. 1995. Microscale force transducer system to quantify isolated heart cell contractile characteristics. *Sens. Actuators A* 26(1-3):233-36
 56. Costin JA. 1994. *US Patent No.* 5279547
 57. Judy JW, Polla DL, Robbins WP. 1990. A linear piezoelectric stepper motor with sub-micrometer displacement and centimeter travel. *IEEE Trans. Ultrason. Ferroelectr. Freq. Control* 37:428-37
 58. Peichel D. 2000. Piezoelectric stepper motor. *J. Microelectromech. Syst.* 37:In press
 59. Robbins WP, Polla DL, Glumac DE. 1991. High displacement piezoelectric actuator using a meander line geometry. I. Experimental characterization. *IEEE Trans. Ultrason. Ferroelectr. Freq. Control* 38(5):454-60
 60. Robbins WP. 1991. High displacement piezoelectric actuator using a meander line geometry. II. Theory. *IEEE Trans. Ultrason. Ferroelectr. Freq. Control* 38(5):461-67
 61. Diaz JA, Gentry WR, Giese CF, Polla DL. 2000. Sub-miniature double-focusing sector field mass spectrometer for in situ gas monitoring. *Proc. Sanibel Conf. Mass Spectrometry: Field Portable Miniature Mass Spectrometry, 12th, Sanibel Island, FL*, p. 6. Am. Soc. Mass Spectrometry
 62. Wang X-B, Huang Y, Vykoukal J, Becker FF, Gascoyne PRC. 2000. Cell separation by dielectrophoretic field-flow-fractionation. *Anal. Chem.* 72(4):832-39
 63. Huang Y, Wang X-B, Becker FF, Gascoyne PR. 1997. Introducing dielectrophoresis as a new force-field for field-flow fractionation. *Biophys. J.* 73:1118-29
 64. Polla DL. 1999. Medical applications of microelectromechanical systems (MEMS). *Int. Conf. Next Gener. Mater. Devices Si-Based Electron., Shanghai, China*
 65. Henry S, McAllister DV, Allen MG, Prausnitz MR. 1998. Microfabricated microneedles: a novel approach to transdermal drug-delivery. *J. Pharm. Sci.* 87(8):922-25
 66. Potts RO, Guy RH, eds. 1997. *Mechanisms of Transdermal Drug Delivery*. New York: Marcel Dekker
 67. Hadgraft J, Guy RH, eds. 1989. *Transdermal Drug Delivery: Developmental Issues and Research Initiatives*. New York: Marcel Dekker
 68. Foreman MI, Clanachan I, Kelly IP. 1983. Diffusion barriers in skin: a new method of comparison. *Br. J. Dermatol.* 108:549-53



CONTENTS

PIERRE M. GALLETTI: A Personal Reflection, <i>Robert M. Nerem</i>	1
PHYSICOCHEMICAL FOUNDATIONS AND STRUCTURAL DESIGN OF HYDROGELS IN MEDICINE AND BIOLOGY, <i>N. A. Peppas, Y. Huang, M. Torres-Lugo, J. H. Ward, J. Zhang</i>	9
BIOENGINEERING MODELS OF CELL SIGNALING, <i>Anand R. Asthagiri, Douglas A. Lauffenburger</i>	31
FUNDAMENTALS OF IMPACT BIOMECHANICS: Part I - Biomechanics of the Head, Neck, and Thorax, <i>Albert I. King</i>	55
INJURY AND REPAIR OF LIGAMENTS AND TENDONS, <i>Savio L.-Y. Woo, Richard E. Debski, Jennifer Zeminski, Steven D. Abramowitch, Serena S. Chan Saw, MS, James A. Fenwick</i>	83
ELECTROPHYSIOLOGICAL MODELING OF CARDIAC VENTRICULAR FUNCTION: From Cell to Organ, <i>R. L. Winslow, D. F. Scollan, A. Holmes, C. K. Yung, J. Zhang, M. S. Jafri</i>	119
CRYOSURGERY, <i>Boris Rubinsky</i>	157
CELL MECHANICS: Mechanical Response, Cell Adhesion, and Molecular Deformation, <i>Cheng Zhu, Gang Bao, Ning Wang</i>	189
MICROENGINEERING OF CELLULAR INTERACTIONS, <i>Albert Folch, Mehmet Toner</i>	227
QUANTITATIVE MEASUREMENT AND PREDICTION OF BIOPHYSICAL RESPONSE DURING FREEZING IN TISSUES, <i>John C. Bischof</i>	257
MICROFABRICATED MICRONEEDLES FOR GENE AND DRUG DELIVERY, <i>Devin V. McAllister, Mark G. Allen, Mark R. Prausnitz</i>	289
CURRENT METHODS IN MEDICAL IMAGE SEGMENTATION, <i>Dzung L. Pham, Chenyang Xu, Jerry L. Prince</i>	315
ANTIBODY ENGINEERING, <i>Jennifer Maynard, George Georgiou</i>	339
NEW CURRENTS IN ELECTRICAL STIMULATION OF EXCITABLE TISSUES, <i>Peter J. Bassar, Bradley J. Roth</i>	377
TWO-PHOTON EXCITATION FLUORESCENCE MICROSCOPY, <i>Peter T. C. So, Chen Y. Dong, Barry R. Masters, Keith M. Berland</i>	399
IMAGING THREE-DIMENSIONAL CARDIAC FUNCTION, <i>W. G. O'Dell, A. D. McCulloch</i>	431
THREE-DIMENSIONAL ULTRASOUND IMAGING, <i>Aaron Fenster, Donal B. Downey</i>	457
BIOPHYSICAL INJURY MECHANISMS IN ELECTRICAL SHOCK TRAUMA, <i>Raphael C. Lee, Dajun Zhang, Jurgen Hannig</i>	477
WAVELETS IN TEMPORAL AND SPATIAL PROCESSING OF BIOMEDICAL IMAGES, <i>Andrew F. Laine</i>	511

MICRODEVICES IN MEDICINE, <i>Dennis L. Polla, Arthur G. Erdman, William P. Robbins, David T. Markus, Jorge Diaz-Diaz, Raed Rizq, Yunwoo Nam, Hui Tao Brickner, Amy Wang, Peter Krulevitch</i>	551
NEUROENGINEERING MODELS OF BRAIN DISEASE, <i>Leif H. Finkel</i>	577
EXTRACORPOREAL TISSUE ENGINEERED LIVER-ASSIST DEVICES, <i>Emmanouhl S. Tzanakakis, Donavon J. Hess, Timothy D. Sielaff, Wei-Shou Hu</i>	607
MAGNETIC RESONANCE STUDIES OF BRAIN FUNCTION AND NEUROCHEMISTRY, <i>Kâmil Ugurbil, Gregor Adriany, Peter Andersen, Wei Chen, Rolf Gruetter, Xiaoping Hu, Hellmut Merkle, Dae-Shik Kim, Seong-Gi Kim, John Strupp, Xiao Hong Zhu, Seiji Ogawa</i>	633
INTERVENTIONAL AND INTRAOPERATIVE MAGNETIC RESONANCE IMAGING, <i>J. Kettenbach, D. F. Kacher, S. K. Koskinen, Stuart G. Silverman, A. Nabavi, Dave Gering, Clare M. C. Tempny, R. B. Schwartz, R. Kikinis, P. M. Black, F. A. Jolesz</i>	661
CARTILAGE TISSUE REMODELING IN RESPONSE TO MECHANICAL FORCES, <i>Alan J. Grodzinsky, Marc E. Levenston, Moonsoo Jin, Eliot H. Frank</i>	691
IN VIVO NEAR-INFRARED SPECTROSCOPY, <i>Peter Rolfe</i>	715